Numerical Investigations on Crack Identification in High-Temperature Superconducting Film*)

Atsushi KAMITANI, Teruou TAKAYAMA, Soichiro IKUNO[1)] and Hiroaki NAKAMURA[2)]

Yamagata University, Yamagata 992-8510, Japan
[1)]*Tokyo University of Technology, Tokyo 192-0982, Japan*
[2)]*National Institute for Fusion Science, Gifu 509-5292, Japan*

(Received 15 November 2013 / Accepted 25 April 2014)

The applicability of the scanning permanent-magnet method (SPM) to the crack identification in a high-temperature superconducting (HTS) film is investigated numerically. To this end, a defect parameter is defined for characterizing a crack position and it is calculated along various scanning lines. The results of computations show that a crack position can be roughly identified by scanning an HTS film in two opposite directions. Hence, the SPM must be combined with the inductive method to develop a fast high-resolution method for identifying a crack.

Keywords: critical current density, high temperature superconductor, integrodifferential equation, surface crack

DOI: 10.1585/pfr.9.3405085

1. Introduction

As is well known, the critical current density j_C is one of the most important parameters for engineering applications of high-temperature superconducting (HTS) films. In this sense, contactless methods have been desired for measuring j_C of HTS films [1, 2].

Ohshima *et al.* [3, 4] proposed the permanent-magnet method for contactlessly measuring j_C of an HTS film. While bringing a permanent magnet closer to an HTS film, they measured the electromagnetic force acting on the film. Consequently, they found that the maximum repulsive force F_M is roughly proportional to j_C. This tendency implies that j_C can be estimated from the measured value of F_M. This is the basic idea of the permanent-magnet method.

Although the permanent-magnet method can be applied not only to the j_C-measurement [3] but also to the crack detection [4], it is extremely time-consuming. This is mainly because F_M must be determined at each measurement point. For the purpose of resolving this problem, Hattori *et al.* [5] improved the permanent-magnet method. In the improved method, the magnet is moved along the film surface and, simultaneously, the electromagnetic force F_z acting on the film is measured. As a result, the j_C-distribution can be successfully determined from the measured F_z-distribution. Throughout the present study, the improved method is called the scanning permanent-magnet method (SPM).

The authors performed the numerical simulation of the SPM. As a result, they showed that the SPM can be applied to the measurement of the j_C-distribution [6]. However, it is not clear whether or not cracks can be identified by using the SPM.

The purpose of the present study is to numerically investigate the applicability of the SPM to the crack identification in an HTS film.

2. Governing Equations

2.1 Scanning permanent-magnet method

A schematic view of the SPM is shown in Fig. 1. A permanent magnet of radius R and height H is placed just above an HTS film of thickness b so that its symmetry axis may be vertical to the film surface. While the distance L between the magnet bottom and the film surface is kept constant, the permanent magnet is moved along the film surface at a constant speed. During the movement of the permanent magnet, an electromagnetic force acting on the

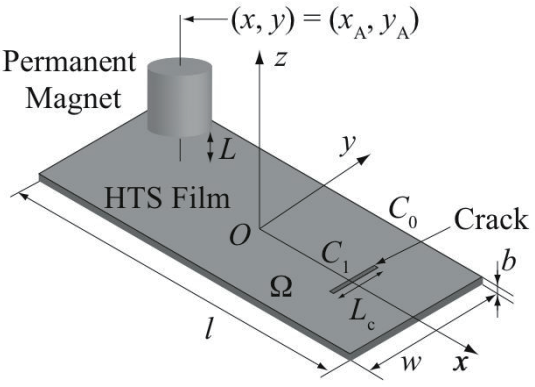

Fig. 1 A schematic view of the SPM.

author's e-mail: kamitani@yz.yamagata-u.ac.jp

*) This article is based on the presentation at the 23rd International Toki Conference (ITC23).

film is monitored.

By taking the thickness direction of the film as z-axis and choosing the centroid of the film as the origin, we use the Cartesian coordinate system $\langle O : \boldsymbol{e}_x, \boldsymbol{e}_y, \boldsymbol{e}_z \rangle$. In terms of the coordinate system, the symmetry axis of the permanent magnet is expressed as $(x, y) = (x_\mathrm{A}, y_\mathrm{A})$.

We first assume that the HTS film has a rectangular cross section Ω of length l and width w. Furthermore, we assume that it contains a crack whose cross section is a line segment connecting two points, $(x_\mathrm{c}, y_\mathrm{c} \pm L_\mathrm{c}/2)$, in the xy plane. Note that the boundary $\partial\Omega$ of Ω is composed of not only the outer boundary C_0 but also the inner boundary C_1. Apparently, C_1 is the crack surface. In the following, $\boldsymbol{t}$ and $\boldsymbol{n}$ denote a unit tangent vector and a unit normal vector on $\partial\Omega$, respectively. Furthermore, $\boldsymbol{x}$ and $\boldsymbol{x}'$ are position vectors of two points in the xy plane.

We further assume that the HTS film is scanned with the permanent magnet in opposite two directions. Specifically, the movements of the magnet are assumed as $x_\mathrm{A} = \pm(vt - l/2) \equiv x_\pm(t)$, where v is a scanning speed.

2.2 Initial-boundary-value problem

As is well known, the electric field $\boldsymbol{E}$ and the shielding current density $\boldsymbol{j}$ are closely related to each other in an HTS film. As the relation, the following power law [7–10] is assumed:

$$\boldsymbol{E} = E(|\boldsymbol{j}|)\,[\boldsymbol{j}/|\boldsymbol{j}|], \quad E(j) = E_\mathrm{C}(j/j_\mathrm{C})^N, \tag{1}$$

where E_C denotes the critical electric field and N is a positive constant.

Under the thin-plate approximation, there exists a scalar function $T(\boldsymbol{x}, t)$ such that $\boldsymbol{j} = (2/b)[\nabla \times (T\boldsymbol{e}_z)]$, and its time evolution is governed by the following integrodifferential equation [10, 11]:

$$\mu_0 \partial_t(\hat{W}T) + \boldsymbol{e}_z \cdot (\nabla \times \boldsymbol{E}) = -\partial_t \langle \boldsymbol{B} \cdot \boldsymbol{e}_z \rangle. \tag{2}$$

Here, $\boldsymbol{B}/\mu_0$ is the magnetic field generated by the permanent magnet. In addition, $\langle\ \rangle$ denotes an average operator over the thickness and $\hat{W}$ is the operator defined by

$$\hat{W}T \equiv \frac{2T(\boldsymbol{x}, t)}{b} + \iint_\Omega Q(|\boldsymbol{x} - \boldsymbol{x}'|)\, T(\boldsymbol{x}', t)\, \mathrm{d}^2\boldsymbol{x}',$$

where $Q(r) = -(\pi b^2)^{-1}[r^{-1} - (r^2 + b^2)^{-1/2}]$. Incidentally, the method for calculating $\boldsymbol{B}/\mu_0$ is described in Appendix.

The initial and boundary conditions to (2) are assumed as follows:

$$T = 0 \ \text{ at } \ t = 0, \tag{3}$$

$$T = 0 \ \text{ on } \ C_0, \tag{4}$$

$$\frac{\partial T}{\partial s} = 0 \ \text{ on } \ C_1, \tag{5}$$

$$\oint_{C_1} \boldsymbol{E} \cdot \boldsymbol{t}\, \mathrm{d}s = 0, \tag{6}$$

where s is an arclength along the crack surface C_1. Equations (4) and (5) are derived from the boundary condition $\boldsymbol{j} \cdot \boldsymbol{n} = 0$ on $\partial\Omega$, whereas (6) is required for the uniqueness of the solution [10].

By solving the initial-boundary-value problem of (2), we can determine the time evolution of the shielding current density. Throughout the present study, the geometrical and physical parameters are fixed as follows: R = 1 mm, H = 2 mm, L = 0.5 mm, B_F = 0.1 T, v = 2 mm/s, E_C = 1 mV/m, j_C = 1.5 MA/cm^2, N = 20, b = 1 μm, l = 30 mm, w = 10 mm, L_c = 2 mm, and $(x_\mathrm{c}, y_\mathrm{c})$ = (3 mm, 0 mm). Here, B_F is the magnitude of the magnetic flux density at $(x, y, z) = (x_\mathrm{A}, y_\mathrm{A}, b/2)$ for the case where the permanent magnet is not moved along the film, and it is employed as a measure of a permanent-magnet strength.

3. Numerical Simulation

For the purpose of solving the initial-boundary-value problem of (2), the authors proposed the virtual voltage method [10, 11]. The basic idea of the method is to apply a virtual voltage along the crack surface to have the integral form (6) of Faraday's law numerically satisfied. The details of the virtual voltage method are described in [10].

On the basis of the virtual voltage method, a numerical code was developed for analyzing the time evolution of the shielding current density in an HTS film with a crack. In the code, a crack is treated as a set of element boundaries and, hence, its size L_c strongly depends on the element division. By executing the code, we can easily evaluate the electromagnetic force F_z acting on the HTS film. In this section, we numerically investigate the following two points:

- How is the SPM affected by a crack?
- Is the SPM applicable to the crack detection?

3.1 Influence of crack on SPM

Let us first investigate the influence of a crack on the electromagnetic force F_z. To this end, dependences of F_z on the scanning position x_A are numerically determined not only for an HTS film with a crack but for an HTS film without a crack. The results of computations are depicted in Fig. 2. This figure indicates that, for $x_\mathrm{A} \lesssim 0$ mm or 12 mm $\lesssim x_\mathrm{A}$, two F_z-x_A curves overlap with each other. Otherwise, two curves show quite different behaviors. This result suggests that the vicinity of the crack is characterized by the force difference $\Delta F_z \equiv F_z^\mathrm{with} - F_z^\mathrm{without}$. Here, F_z^with and F_z^without are the electromagnetic forces F_z for an HTS film with and without a crack, respectively.

The dependence of ΔF_z on x_A is numerically determined and is depicted in the inset of Fig. 2. We see from this inset that, if the inequality $|x_\mathrm{A} - x_\mathrm{c}| \lesssim 3$ mm is satisfied, namely, if the scanning position is located near the crack, the force difference ΔF_z shows a violent change. In addition, $|\Delta F_z|$ almost vanishes for $x_\mathrm{A} - x_\mathrm{c} \lesssim -3$ mm, whereas it still remains relatively large for 3 mm $\lesssim x_\mathrm{A} - x_\mathrm{c} \lesssim 9$ mm. In other words, the ΔF_z-x_A curve is neither symmetric nor antisymmetric with respect to $x_\mathrm{A} = x_\mathrm{c}$.

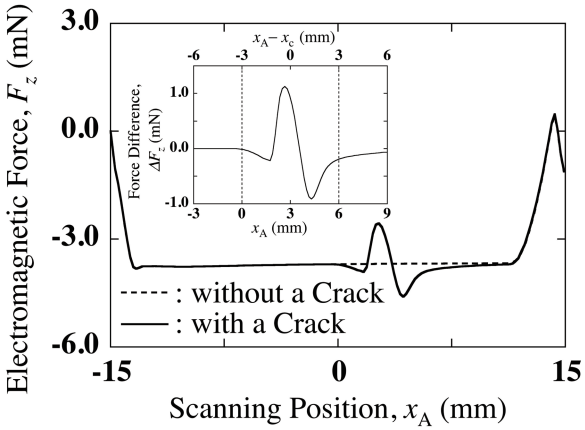

Fig. 2 Dependences of the electromagnetic force F_z on the scanning position x_A. Here, the movement of of the magnet is assumed as $x_A = x_+(t)$ and $y_A = 0$ mm. The inset shows the dependence of the force difference ΔF_z on x_A for the same case.

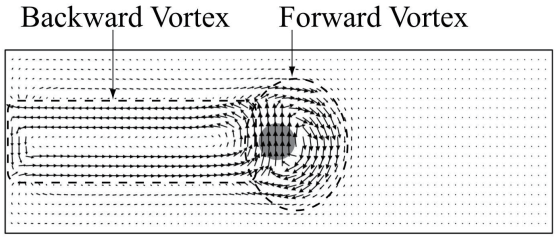

Fig. 3 The $\boldsymbol{j}$-distribution in the HTS film without a crack for the case with $x_A = x_+(t)$ and $y_A = 0$ mm. Here, the distribution is obtained at time t satisfying $x_A = -1$ mm. In Figs. 3 and 4, the shaded circular region indicates the projection of the permanent magnet onto the film surface.

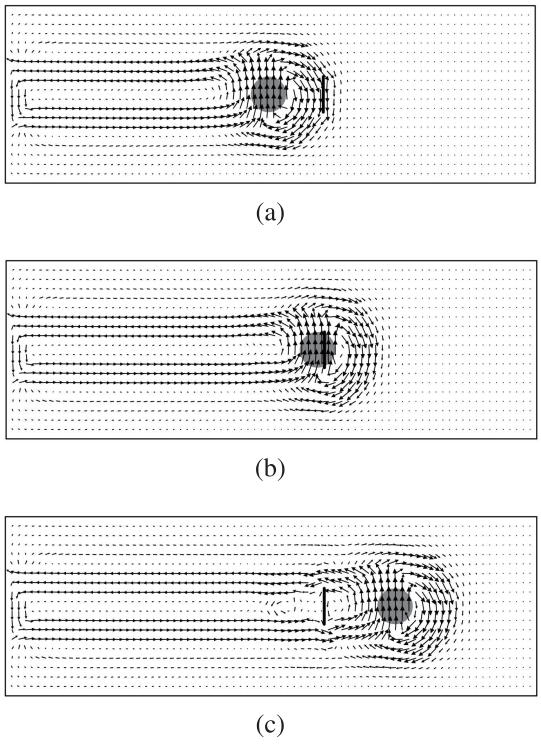

Fig. 4 The $\boldsymbol{j}$-distributions for the case with $x_A = x_+(t)$ and $y_A = 0$ mm. Here, the distributions are obtained at time t satisfying the following conditions: (a) $x_A = -1$ mm, (b) $x_A = 2.6$ mm, and (c) $x_A = 7$ mm. In these figures, cracks are denoted by thick line segments.

Next, we investigate the spatial distributions of the shielding current density $\boldsymbol{j}$ to explain the asymmetric behavior of the ΔF_z-x_A curve. For the HTS film without a crack, the $\boldsymbol{j}$-distribution is roughly composed of two current vortices: a forward current vortex forms an almost circular flow pattern, whereas a backward current vortex shows an oblately ellipsoidal one (see Fig. 3). As the permanent magnet is moved along the film surface, these two vortices shift with their flow patters unchanged. In the following, these two vortices are called a forward vortex and a backward one.

For the HTS film containing a crack, slightly different $\boldsymbol{j}$-distributions are observed. The crack hardly affects the $\boldsymbol{j}$-distribution for $x_A = -1$ mm ($x_A - x_c = -4$ mm) (see Fig. 4 (a)). Furthermore, the crack perturbs only the backward vortex for $x_A = 7$ mm ($x_A - x_c = 4$ mm) (see Fig. 4 (c)), whereas only the forward vortex is remarkably deformed for $x_A = 2.6$ mm ($x_A - x_c = -0.4$ mm) (see Fig. 4 (b)). These results indicate that, for $x_A - x_c \lesssim -3$ mm, the crack has influence on neither the forward vortex nor the backward one. In addition, the crack disturbs only the backward vortex for 3 mm $\lesssim x_A - x_c \lesssim 9$ mm, whereas it deforms only the forward vortex for $|x_A - x_c| \lesssim 3$ mm. In this way, an asymmetric behavior of the ΔF_z-x_A curve is caused by the deformation of a forward/backward vortex.

3.2 Crack identification using SPM

As mentioned above, $|\Delta F_z|$ takes a relatively large value only when either a forward vortex or a backward one is disturbed by a crack. The forward vortex is disturbed if the scanning position x_A is located near the crack position x_c. On the other hand, the backward vortex is disturbed unless $x_A - x_c$ exceeds several times the radius R of the permanent magnet. Hence, when $|\Delta F_z|$ does not vanish due to the disturbed forward vortex, the scanning position x_A can be regarded as a rough estimation of the crack position x_c. In order to extract the scanning position x_A at which only the forward vortex is disturbed, we define the following defect parameter: $d \equiv \mathrm{sgn}(\Delta F_z^+ \cdot \Delta F_z^-)\sqrt{|\Delta F_z^+ \cdot \Delta F_z^-|}$. Here, ΔF_z^+ and ΔF_z^- denote the force difference for $x_A = x_+(t)$ and that for $x_A = x_-(t)$, respectively, and both of them are obtained by scanning an HTS film in two opposite directions.

The defect parameter d is calculated as functions of the scanning position x_A and is depicted in Fig. 5. As expected, $|d|$ takes a large value only for $x_A \cong x_c$ and it rapidly decreases with an increase in $|x_A - x_c|$. In other words, a crack can be found in the region where $|d|$ ex-

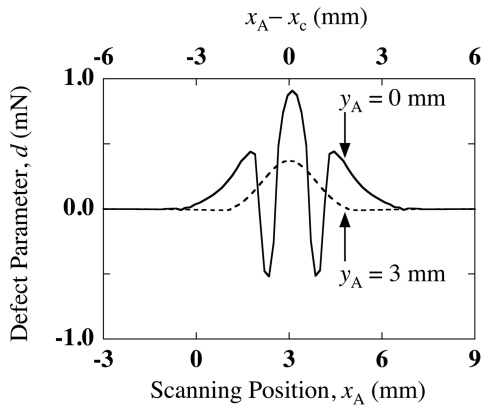

Fig. 5 Dependences of the defect parameter d on the scanning position x_A.

ceeds a small positive constant α. On the basis of this result, we can approximately determine the region D_c in which a crack is contained. The method for determining D_c is composed of the following two steps:

1. The shortest single interval $I(y_A)$ such that

$$I(y_A) \supseteq \{x_A : |x_A| < l/2, |d(x_A, y_A)| > \alpha\},$$

is numerically determined. Here, α is a sufficiently small threshold. Incidentally, for $x_A \in I(y_A)$, a deformed forward vortex is always observed.
2. The region D_c is determined by using

$$D_c = \{(x_A, y_A) : x_A \in I(y_A), |y_A| < w/2\}.$$

By means of the above two steps, the region D_c is numerically determined in the 1st and 2nd quadrants of the xy-plane. The boundary ∂D_c of the region D_c is depicted in Fig. 6. The contours of the defect parameter d are also shown in this figure. Since the cross section of the crack is assumed to be a line segment of length 2 mm, it is completely contained in D_c. In other words, a crack can be identified by means of the SPM. However, the area of D_c is relatively large as compared with that of the HTS film. Hence, the SPM shows only a low resolution in the crack identification. These results indicate that, although the SPM is applicable to the crack identification, its resolution is not satisfactory enough as compared with that of the inductive method [1, 2, 11]. On the other hand, the measurement time of the SPM is much shorter than that of the inductive method. In this sense, we should combine both methods to develop a high-performance method for identifying a crack. In the resulting method, the region D_c containing a crack is first estimated by using the SPM and, subsequently, the crack is accurately identified by applying the inductive method only in D_c.

4. Conclusion

We have numerically investigated the influence of a crack on the SPM and have also assessed the applicability

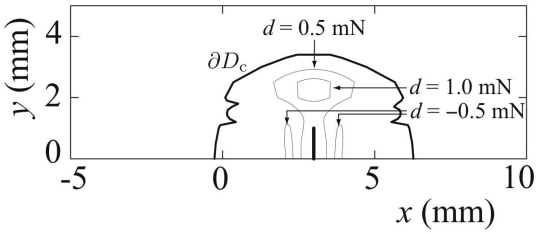

Fig. 6 The boundary ∂D_c of the region D_c and contours of the defect parameter d. Here, α is fixed as $\alpha = 2 \times 10^{-2}$ mN. In this figure, a crack is denoted by a thick line segment.

of the SPM to the crack identification.

Conclusions obtained in the present study are summarized as follows:

1. The defect parameter d can be determined by scanning an HTS film in two opposite directions. It changes violently only when the permanent magnet is moving just near a crack. In this sense, d can be adopted as a suitable parameter for detecting a crack.
2. The SPM shows a much lower resolution than the inductive method and, hence, it is effective only in the rough identification of a crack.

Acknowledgment

This work was supported in part by Japan Society for the Promotion of Science under a Grant-in-Aid for Scientific Research (C) No. 24560321. A part of this work was also carried out with the support and under the auspices of the NIFS Collaboration Research program (NIFS13KNTS025, NIFS13KNXN267).

Appendix

In this appendix, we explain the method for calculating the magnetic field $\boldsymbol{B}_0/\mu_0$ generated by a cylindrical permanent magnet of radius R and height H.

By taking the symmetry axis of the magnet as z-axis and choosing $A(x_A, y_A, 0)$ as the origin, we also use the cylindrical coordinate system $\langle A : \boldsymbol{e}_r, \boldsymbol{e}_\theta, \boldsymbol{e}_z \rangle$. In the following, $\boldsymbol{z}$ and $\boldsymbol{z}'$ denote position vectors of two points in the xyz space. Furthermore, the cylindrical coordinates of $\boldsymbol{z}$ and $\boldsymbol{z}'$ are denoted by (r, θ, z) and (r', θ', z'), respectively.

As is well known, the magnetic vector potential $\boldsymbol{A}(\boldsymbol{z})$ generated by the magnetization $\boldsymbol{M}(\boldsymbol{z})$ is given by

$$\boldsymbol{A}(\boldsymbol{z}) = \frac{\mu_0}{4\pi}\Big[\iiint_V \frac{\nabla' \times \boldsymbol{M}(\boldsymbol{z}')}{|\boldsymbol{z} - \boldsymbol{z}'|} \, \mathrm{d}^3 z' + \iint_{\partial V} \frac{\boldsymbol{M}(\boldsymbol{z}') \times \boldsymbol{n}(\boldsymbol{z}')}{|\boldsymbol{z} - \boldsymbol{z}'|} \, \mathrm{d}S(\boldsymbol{z}') \Big], \quad \text{(A.1)}$$

where V and ∂V are the permanent magnet and its surface, respectively, and $\boldsymbol{n}(\boldsymbol{z}')$ denotes an outward unit normal on ∂V.

In the present study, we assume that the magnetization $\boldsymbol{M}(\boldsymbol{z})$ is uniform in V and that it is parallel to the symmetry

axis of the permanent magnet. In other words, $\boldsymbol{M}(z)$ is assumed to satisfy $\boldsymbol{M}(z) = M\boldsymbol{e}_z$, where M is a constant.

Under these assumptions, the vector potential $\boldsymbol{A}(z)$ can be rewritten in the form,

$$\boldsymbol{A}(z) = \frac{\mu_0 M}{2\pi}\sqrt{\frac{R}{r}}\,\boldsymbol{e}_\theta \times \int_{z_1}^{z_2} k\left[\left(\frac{2}{k^2}-1\right)\mathrm{K}(k) - \frac{2\mathrm{E}(k)}{k^2}\right]\mathrm{d}z', \quad \text{(A.2)}$$

where $z_j = b/2 + L + (j-1)H$ $(j = 1, 2)$. In addition, $\mathrm{K}(k)$ and $\mathrm{E}(k)$ are the complete elliptic integrals of the first and second kinds, respectively, and their parameter k is given by $k^2 = 4rR/[(r+R)^2 + (z-z')^2]$.

By substituting (A.2) into $\boldsymbol{B} = \nabla \times \boldsymbol{A}$, we can easily calculate the magnetic field $\boldsymbol{B}/\mu_0$ generated by the permanent magnet.

[1] J.H. Claassen, M.E. Reeves and R.J. Soulen, Jr., Rev. Sci. Instrum. **62**, 996 (1991).

[2] Y. Mawatari, H. Yamasaki and Y. Nakagawa, Appl. Phys. Lett. **81**, 2424 (2002).

[3] S. Ohshima, K. Takeishi, A. Saito, M. Mukaida, Y. Takano, T. Nakamura, I. Suzuki and M. Yokoo, IEEE Trans. Appl. Supercond. **15**, 291 (2005).

[4] S. Ohshima, K. Umezu, K. Hattori, H. Yamada, A. Saito, T. Takayama, A. Kamitani, H. Takano, T. Suzuki, M. Yokoo and S. Ikuno, IEEE Trans. Appl. Supercond. **21**, 3385 (2011).

[5] K. Hattori, A. Saito, Y. Takano, T. Suzuki, H. Yamada, T. Takayama, A. Kamitani and S. Ohshima, Physica C **471**, 1033 (2011).

[6] T. Takayama, A. Saitoh and A. Kamitani, IEEE Trans. Appl. Supercond. **22**, 4903904 (2012).

[7] R. Fresa, G. Rubinacci, S. Ventre, F. Villone and W. Zamboni, IEEE Trans. Magn. **45**, 988 (2009).

[8] R. Brambilla, F. Grilli and L. Martini, IEEE Trans. Appl. Supercond. **22**, 8401006 (2012).

[9] A. Kameni, J. Lambrechts, J.F. Remacle, S. Mezani, F. Bouillault and C. Geuzaine, IEEE Trans. Magn. **48**, 591(2012).

[10] A. Kamitani, T. Takayama and S. Ikuno, IEEE Trans. Magn. **49**, 1877 (2013).

[11] A. Kamitani, T. Takayama and S. Ikuno, Physica C **494**, 168 (2013).